

Research Article

Multishelled NiO Hollow Spheres Decorated by Graphene Nanosheets as Anodes for Lithium-Ion Batteries with Improved Reversible Capacity and Cycling Stability

Lihua Chu,¹ Meicheng Li,^{1,2} Yu Wang,¹ Xiaodan Li,¹ Zipei Wan,¹ Shangyi Dou,¹ and Yue Chu¹

¹State Key Laboratory of Alternate Electrical Power System with Renewable Energy Sources, North China Electric Power University, Beijing 102206, China

²Chongqing Materials Research Institute, Chongqing 400707, China

Correspondence should be addressed to Meicheng Li; mcli@ncepu.edu.cn

Received 15 December 2015; Revised 16 January 2016; Accepted 21 April 2016

Academic Editor: Raul Arenal

Copyright © 2016 Lihua Chu et al. This is an open access article distributed under the Creative Commons Attribution License, which permits unrestricted use, distribution, and reproduction in any medium, provided the original work is properly cited.

Graphene-based nanocomposites attract many attentions because of holding promise for many applications. In this work, multishelled NiO hollow spheres decorated by graphene nanosheets nanocomposite are successfully fabricated. The multishelled NiO microspheres are uniformly distributed on the surface of graphene, which is helpful for preventing aggregation of as-reduced graphene sheets. Furthermore, the NiO/graphene nanocomposite shows much higher electrochemical performance with a reversible capacity of 261.5 mAh g⁻¹ at a current density of 200 mA g⁻¹ after 100 cycles tripled compared with that of pristine multishelled NiO hollow spheres, implying the potential application in modern science and technology.

1. Introduction

With the rapid development of the global economy, fast depletion of nonrenewable energy, and the increasing environmental problems, it is urgent to develop new clean and sustainable sources and technologies for energy storage and conversion with high efficiency [1–3]. Rechargeable lithium-ion batteries (LIBs) are a promising one for the upcoming demand such as electric vehicles and grid storage systems because of their high energy density, long lifespan, and environmental benignancy.

As one of the special structures of carbon, graphene has initiated enormous scientific activities, with the honeycomb lattice structure, unique structural features of chemical stability, high surface area, flexibility, and superior electric and thermal conductivity. It has been used as ideal building blocks for energy storage systems with improved electrochemical properties compared with these host materials, such as metal, metal oxide, and sulfide [4, 5]. To further explore the potential application of graphene-based nanomaterials, deriving from

the decoration of graphene nanosheets (GNS) with nanomaterials attracts more and more interest. So far, several graphene-based nanocomposites have been successfully fabricated and show desirable combinations of properties that are not found in individual components [6, 7].

Nickel oxide (NiO) is one of prospective anode materials in li-ion battery (LIB), which possesses the advantages of high theoretical capacity (717 mAh g⁻¹), high natural abundance, nontoxicity, low cost, and environmental benignity [8–11]. However, the practical utilization of NiO is still limited owing to its poor cycling and rate performances of the NiO-based LIBs. Several strategies have been undertaken to enhance the performance of NiO electrode materials. One well-established method is constructing hybrid with GNS. Various structures of NiO/GNS, such as porous NiO-wrapped GNS [12], 3D-hierarchical NiO/GNS [13], and graphene anchored with nickel nanoparticles [14], have been prepared, revealing that the NiO/GNS nanocomposite reinforces the properties of pristine NiO which favors their wide application in LIBs.

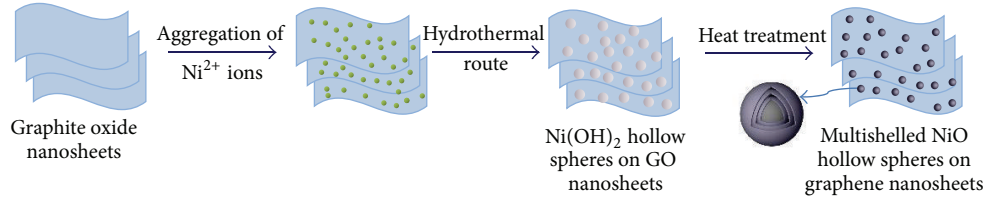


FIGURE 1: Illustration of the procedures for preparation of NiO/graphene hierarchical structure.

In this work, we report the solvothermal method for the synthesis of multishelled NiO hollow spheres/GNS nanocomposite, in which the multishelled NiO hollow spheres are wrapped by GNS. This hybrid architecture is found to display much improved electrochemical properties by comparison to that of pristine multishelled NiO hollow microspheres.

2. Experimental

The composite was prepared by the solvothermal method. 3 mL graphite oxide (6 mol L^{-1}) was ultrasonically dispersed in 30 mL of deionized water and then 1 g of $\text{Ni}(\text{NO}_3)_2 \cdot 6\text{H}_2\text{O}$ and 1 g of D-glucose were added, adjusting the pH to 10.90 with $\text{NH}_3 \cdot \text{H}_2\text{O}$, using a pH meter and magnetic stirrer to form a homogeneous solution at room temperature. The solution was then transferred into a Teflon-lined stainless steel autoclave (50 mL), sealed, and heated at 150°C for 15 h. The product was collected by centrifugation, washed with deionized water several times to remove impurity, and then dried at 60°C in vacuum. Finally, the NiO/graphene was obtained by calcining the precursor in N_2 at 300°C for 2 h and then in air at 500°C for 2 h. For comparison, the multishelled NiO spheres were prepared by a similar solution-based method and subsequent calcination with the absence of graphene oxide (GO).

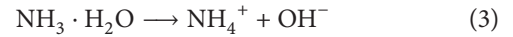
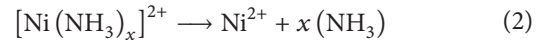
The crystallographic structures, morphology, and microstructure of the as-prepared products were characterized by Bruker D8 Focus X-ray powder diffractometer with using $\text{Cu K}\alpha$ ($\lambda = 1.5406 \text{ \AA}$) radiation over a range of 2θ from 20° to 90° , FEI Quanta 200F microscope field emission scanning electron microscope (FESEM), and Tecnai G2 F20 Field emission transmission electron microscopy (TEM) with accelerating voltage of 200 kV. Raman measurements were recorded on Laser Confocal Micro-Raman Spectroscopy (LabRAM Aramis).

Electrochemical measurements were conducted using a CR-2032-coin type cell configuration. The electrode materials are a slurry consisting of 80 wt% of electrode materials, 10 wt% of acetylene black (Super-P), and 10 wt% of polyvinylidene fluoride (PVDF) dissolved in N-methyl-2-pyrrolidinone. They were coated onto a copper foil and dried at 100°C in vacuum for 12 h before pressing. Lithium foil was used as the counter and reference electrodes and the polypropylene foil (Celgard 2400) was used as the separator. The electrolyte was 1 M LiPF_6 dissolved in a mixture of ethylene carbonate (EC) and dimethyl carbonate (DMC) (v/v = 1:1). Galvanostatic discharge-charge (GDC) experiments were carried out at different current densities in the voltage

range of 0.01–3.00 V with a multichannel battery tester (Maccor, Inc., USA). Cycling and rate performances were measured by the electrochemical workstation (LAND battery test system).

3. Results and Discussion

A schematic illustration of the fabrication process of NiO/graphene composite is shown in Figure 1. Graphite oxide (GO) was sonicated in di-water to form a homogeneous suspension. Then, the GO nanosheets absorb Ni^{2+} ions, which react with OH^- to grow $\text{Ni}(\text{OH})_2$ architectures on GO nanosheets. Here, OH^- were released by $\text{NH}_3 \cdot \text{H}_2\text{O}$, which can also control the morphology of the $\text{Ni}(\text{OH})_2$ architectures. The formation of $\text{Ni}(\text{OH})_2$ from Ni^{2+} ions and $\text{NH}_3 \cdot \text{H}_2\text{O}$ can be expressed by the following reactions:



During the calcination, $\text{Ni}(\text{OH})_2$ decomposed to yield multishelled NiO hollow spheres following $\text{Ni}(\text{OH})_2 \rightarrow \text{NiO} + \text{H}_2\text{O}$, and GO nanosheets reduced to graphene by losing oxygen-containing surface groups [15, 16]. So the $\text{Ni}(\text{OH})_2/\text{GO}$ precursor converted to NiO/GNS composites after annealing. The pristine multishelled NiO hollow spheres would be obtained without GO during the similar reaction process, which were discussed in our previous paper [17].

The XRD patterns of NiO and NiO/GNS composite are shown in Figure 2(a). All of the diffraction peaks of pure NiO sample can be ascribed to face centered cubic NiO (JCPDS number 071-1179), which correspond to (111), (200), (220), (311), and (222) planes, respectively. All the characteristic peaks of pure NiO are also observed for NiO/GNS composite. (002) diffraction peak of GNS is typically located at about 24° in the XRD pattern, but it is not obvious in Figure 2(a). Because the content of graphene is low and the diffraction of disorderedly stacked GNS is quite weaker as compared to the well-crystalline NiO, the presence of graphene can be confirmed in the Raman spectra of NiO/GNS, as shown in Figure 2(b), where the G characteristic peaks of graphene are obvious, though the D peak located at $\sim 1350 \text{ cm}^{-1}$ is invisible.

The morphology of pristine NiO and NiO/GNS composite is compared by SEM and TEM. Pure NiO is composed of

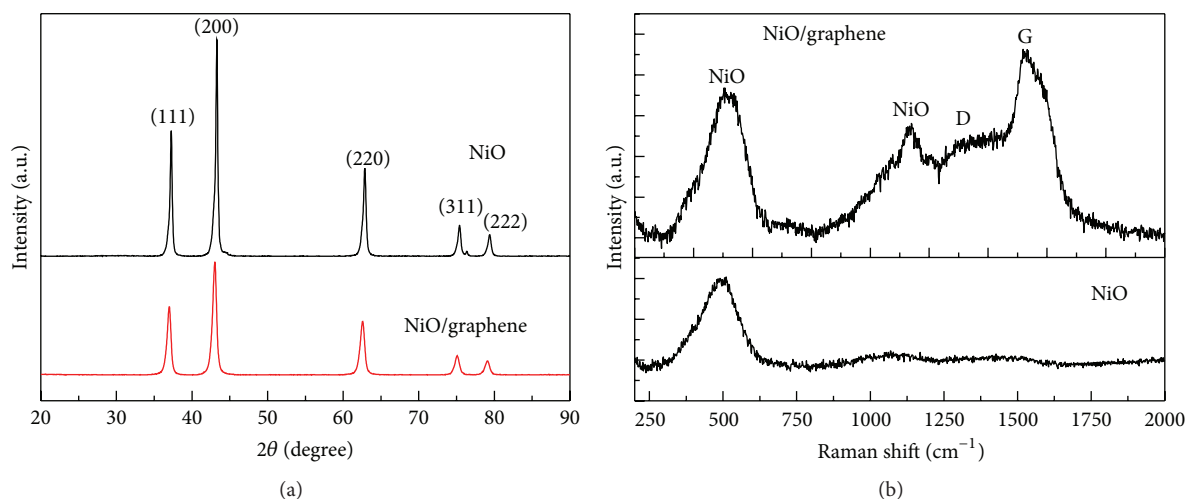


FIGURE 2: (a) X-ray diffraction patterns and (b) Raman spectra for pristine NiO and NiO/graphene composite.

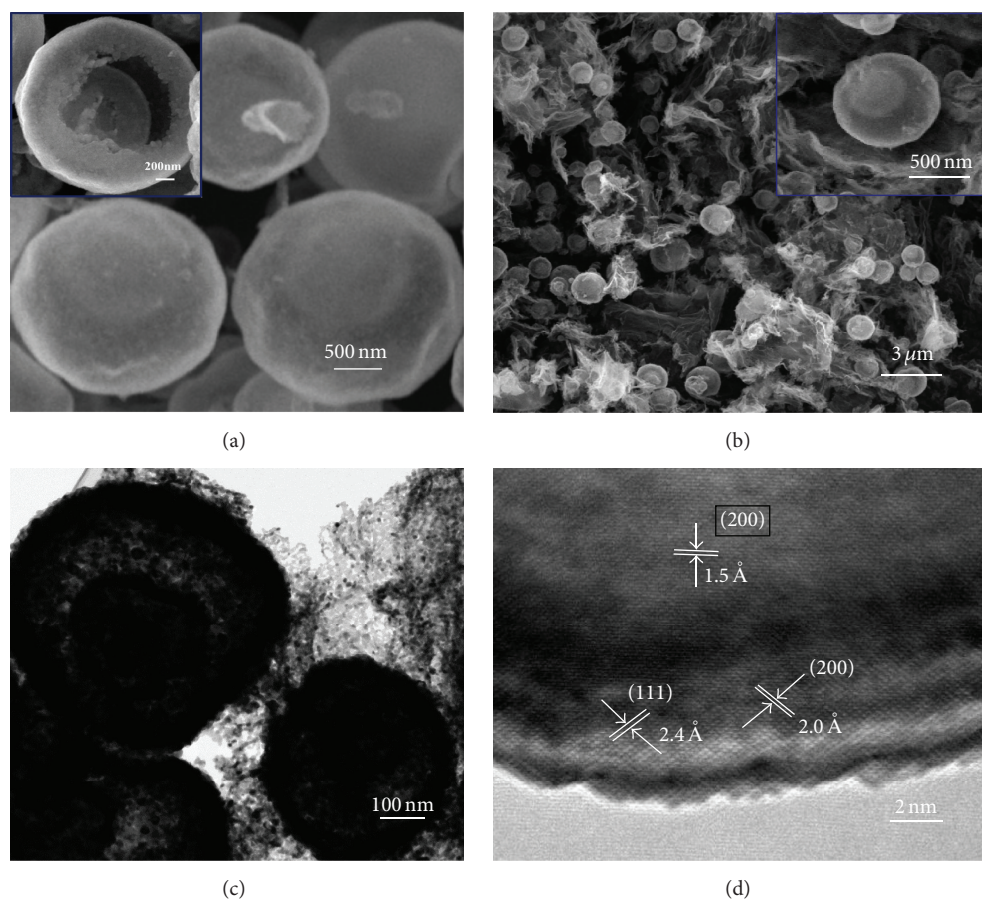


FIGURE 3: SEM images of pristine multishelled NiO spheres (a), NiO/graphene (b), TEM images of NiO/graphene (c), and HRTEM pattern of multishelled NiO spheres (d).

multishelled spheres as shown in Figure 3(a). The NiO/GNS are composed of typical rippled and crumpled GNS and multishelled NiO spheres (Figure 3(b)). It can be clearly seen that the multishelled NiO microspheres with diameter varying from 2.0 μm to 3.5 μm are uniformly distributed on

the surface of GNS. The hybrid architecture can effectively prevent the agglomeration of as-reduced GNS. The inset of Figure 3(b) is the multishelled NiO sphere on the GNS which demonstrates that the multishelled NiO spheres do not change after the addition of graphene. Figure 3(c) shows

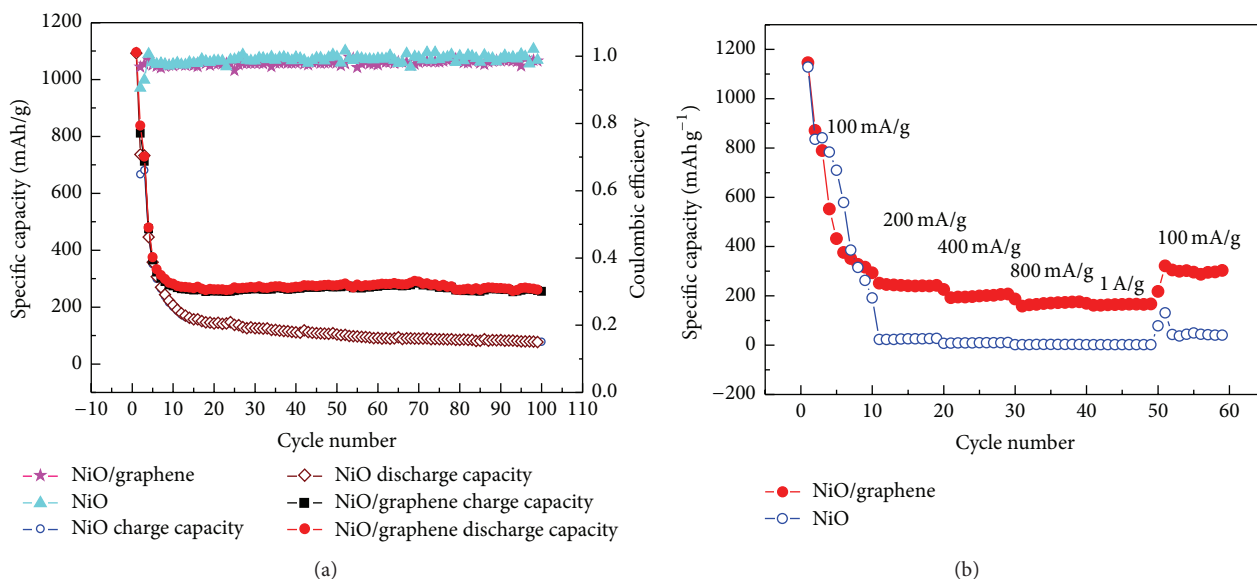


FIGURE 4: (a) Capacity retention and Coulombic efficiency at a current density of 200 mA g^{-1} . (b) Rate performance at various current densities between 100 mA g^{-1} and 1 A g^{-1} .

the TEM image of NiO/GNS which further confirms the multishelled sphere feature of NiO. The HRTEM pattern of multishelled NiO sphere is presented in Figure 3(d). The lattice spacing of 0.15, 0.2, and 0.24 nm is observed, corresponding to the interspaces of (220), (200) and (111), and (200) planes of cubic NiO.

The electrochemical properties of NiO/GNS composite were evaluated as anode for lithium-ion batteries (LIBs). Figure 4 displays the cycling and rate performances of NiO/GNS composite and pristine NiO. The initial discharge capacities are $\sim 1100 \text{ mAh g}^{-1}$ as shown in Figure 4(a). It is much higher than the theoretical value (718 mAh g^{-1}), mainly attributed to the solid electrolyte interphase (SEI) film formation, and the additional Li^+ storage in the space between NiO spheres and GNS. The reversible capacity of NiO spheres decreases to 77.1 mAh g^{-1} after 100 cycles. While the reversible capacity of NiO/GNS composite still can retain 261.5 mAh g^{-1} after 100 cycles, which is more than three times of pristine NiO sphere. The coulombic efficiencies increase to and almost keep stable in the scale of 98-99% at successive cycles, indicating that the formed SEI film is favorable and stable [18]. The enhanced cycling performance of NiO/GNS composite should be ascribed to the addition of graphene and the hybrid architecture. Firstly, the GNS have much better conductivity due to the wider layer spacing compared with NiO. The d -spacing of GNS was found to be 0.365 nm, and the maximum d -spacing of NiO is 0.24 nm ((111) lattice plane) [19]. Therefore, the GNS can offer additional sites for accommodation of Li^+ leading to the enhanced reversible capacity. Secondly, the flexible GNS can accommodate the volume change and prevent the aggregation of active materials upon cycling. Thirdly, the hybrid architecture can also be helpful for preventing aggregating or restacking of as-reduced GNS.

Moreover, the NiO/GNS composites also exhibit enhanced rate capacity compared with pristine NiO spheres, as presented in Figure 4(b). The discharge capacities of NiO/GNS at 100 mA g^{-1} , 200 mA g^{-1} , 400 mA g^{-1} , 800 mA g^{-1} , and 1 A g^{-1} are 292.3 mAh g^{-1} (10th cycle), 225.9 mAh g^{-1} (20th cycle), 187.3 mAh g^{-1} (30th cycle), 169.3 mAh g^{-1} (40th cycle), and 166.5 mAh g^{-1} (50th cycle), respectively. In the initial 10 cycles with a small current density (100 mA g^{-1}), the capacities of pristine NiO and NiO/GNS composite are comparable, and the pristine NiO is even a little better than NiO/GNS composite, which may be caused by the lower capacity of graphene as compared to NiO [18]. However, the situation reverses when the current density increases. The enhanced rate capacity could be reasonably attributed to advantageous combination of the highly conductive GNS and the favorable multishelled NiO hollow spheres architecture with large specific surface area and open inner cavity, which can facilitate the rapid diffusion of lithium ions from electrolyte to active material.

As shown in Figure 4(b), the capacity dropped dramatically from $\sim 1100 \text{ mAh g}^{-1}$ to a little more than 300 mAh g^{-1} during the first five cycles with a small current density (100 mA g^{-1}). Generally, the capacity lost in the first several cycles can be attributed to the irreversible reactions involved in the formation of the SEI layer. In addition, the formation and stabilization of the SEI layer are a gradual process, so that stable capacity also requires a process, which has been described in many works [20, 21]. It is also probably caused by large theoretical capacity difference between NiO (717 mAh g^{-1}) and graphene (372 mAh g^{-1}). During the first several cycles, the synergy effect between NiO and graphene does not play well during the lithiation and delithiation process; therefore, the NiO and graphene do not serve well in

terms of improving and stabilizing capacity. So the dropped capacity is due to the formation of SEI layer and the capacity difference in the first several cycles.

The NiO/GNS composite demonstrates improved electrochemical performance, which could be due to several reasons. Firstly, the wider GNS can offer additional sites for the accommodation of Li^+ compared with NiO. Moreover, the well-contact GNS and multishelled NiO hollow spheres can facilitate the continuous and rapid conducting pass way of Li^+ , which are beneficial for enhancing specific capacity and rate performance of the active materials. Secondly, GNS are anticipated to prevent the collapse and aggregation of the active materials upon cycling, which brings about excellent cycling stability. Vice versa, the hybrid architecture can also be helpful for preventing aggregating of GNS [12]. Thirdly, the large specific surface area and open inner cavity of GNS and the favorable multishelled NiO hollow spheres architecture can provide sufficient electrode/electrolyte contact areas and facilitate the continuous and rapid electron transport through the electrodes, resulting in the improved rate performance.

4. Conclusions

In summary, we have successfully fabricated NiO/GNS composite, in which the multishelled NiO microspheres are uniformly distributed on the surface of GNS. The composite shows much enhanced cycling stability and capacity compared with the pristine multishelled NiO hollow spheres, when evaluated as the anode materials in LIBs. The superior performance in LIBs originates from the addition of GNS and the sandwich-like architecture, which can facilitate the continuous and rapid electron transport and prevent the collapse of nanostructures and aggregation of the active materials. The strategies described here could offer an effective method to improve the electrochemical performance of other electrode materials with large volume changes and low electrical conductivities.

Competing Interests

The authors declare that they have no competing interests.

Acknowledgments

This work is supported partially by National High-tech R&D Program of China (863 Program, no. 2015AA034601), National Natural Science Foundation of China (Grant nos. 91333122, 51402106, 51372082, 51172069, 61204064, and 51202067), Ph.D. Programs Foundation of Ministry of Education of China (Grant nos. 20120036120006 and 20130036110012), Par-Eu Scholars Program, and the Fundamental Research Funds for the Central Universities.

References

- [1] H. Xia, C. Hong, X. Shi et al., "Hierarchical heterostructures of Ag nanoparticles decorated MnO_2 nanowires as promising electrodes for supercapacitors," *Journal of Materials Chemistry A*, vol. 3, no. 3, pp. 1216–1221, 2015.
- [2] H. Xia, C. Hong, B. Li et al., "Facile synthesis of hematite quantum dot/functionalized graphene-sheet composites as advanced anode materials for asymmetric supercapacitors," *Advanced Functional Materials*, vol. 25, no. 4, pp. 627–635, 2015.
- [3] H. Xia, D. Zhu, Z. Luo et al., "Hierarchically structured Co_3O_4 @Pt@ MnO_2 nanowire arrays for high-performance supercapacitors," *Scientific Reports*, vol. 3, article 2978, 2013.
- [4] J. Zhu, D. Yang, Z. Yin, Q. Yan, and H. Zhang, "Graphene and graphene-based materials for energy storage applications," *Small*, vol. 10, no. 17, pp. 3480–3498, 2014.
- [5] M. Pumera, "Graphene-based nanomaterials for energy storage," *Energy and Environmental Science*, vol. 4, no. 3, pp. 668–674, 2011.
- [6] C. Zhang, X. Peng, Z. Guo et al., "Carbon-coated SnO_2 /graphene nanosheets as highly reversible anode materials for lithium ion batteries," *Carbon*, vol. 50, no. 5, pp. 1897–1903, 2012.
- [7] D.-H. Lee, J.-C. Kim, H.-W. Shim, and D.-W. Kim, "Highly reversible Li storage in hybrid NiO/Ni/graphene nanocomposites prepared by an electrical wire explosion process," *ACS Applied Materials & Interfaces*, vol. 6, no. 1, pp. 137–142, 2014.
- [8] N. S. Spinner, A. Palmieri, N. Beauregard, L. Zhang, J. Campanella, and W. E. Mustain, "Influence of conductivity on the capacity retention of NiO anodes in Li-ion batteries," *Journal of Power Sources*, vol. 276, pp. 46–53, 2015.
- [9] X. Yan, X. Tong, J. Wang, C. Gong, M. Zhang, and L. Liang, "Synthesis of hollow nickel oxide nanotubes by electrospinning with structurally enhanced lithium storage properties," *Materials Letters*, vol. 136, pp. 74–77, 2014.
- [10] W. Sun, X. Rui, J. Zhu et al., "Ultrathin nickel oxide nanosheets for enhanced sodium and lithium storage," *Journal of Power Sources*, vol. 274, pp. 755–761, 2015.
- [11] D. Mao, J. Yao, X. Lai, M. Yang, J. Du, and D. Wang, "Hierarchically mesoporous hematite microspheres and their enhanced formaldehyde-sensing properties," *Small*, vol. 7, no. 5, pp. 578–582, 2011.
- [12] D. Xie, Q. Su, W. Yuan, Z. Dong, J. Zhang, and G. Du, "Synthesis of porous NiO-wrapped graphene nanosheets and their improved lithium storage properties," *Journal of Physical Chemistry C*, vol. 117, no. 46, pp. 24121–24128, 2013.
- [13] L. Tao, J. Zai, K. Wang et al., "3D-hierarchical NiO-graphene nanosheet composites as anodes for lithium ion batteries with improved reversible capacity and cycle stability," *RSC Advances*, vol. 2, no. 8, pp. 3410–3415, 2012.
- [14] Y. J. Mai, J. P. Tu, C. D. Gu, and X. L. Wang, "Graphene anchored with nickel nanoparticles as a high-performance anode material for lithium ion batteries," *Journal of Power Sources*, vol. 209, pp. 1–6, 2012.
- [15] H. Li, L. Pan, C. Nie, Y. Liu, and Z. Sun, "Reduced graphene oxide and activated carbon composites for capacitive deionization," *Journal of Materials Chemistry*, vol. 22, no. 31, pp. 15556–15561, 2012.
- [16] I. R. M. Kottegoda, N. H. Idris, L. Lu, J.-Z. Wang, and H.-K. Liu, "Synthesis and characterization of graphene-nickel oxide nanostructures for fast charge-discharge application," *Electrochimica Acta*, vol. 56, no. 16, pp. 5815–5822, 2011.
- [17] L. Chu, M. Li, Z. Wan et al., "Morphology control and fabrication of multi-shelled NiO spheres by tuning the pH value via a hydrothermal process," *CrystEngComm*, vol. 16, no. 48, pp. 11096–11101, 2014.
- [18] Y. Huang, X.-L. Huang, J.-S. Lian, D. Xu, L.-M. Wang, and X.-B. Zhang, "Self-assembly of ultrathin porous NiO

- nanosheets/graphene hierarchical structure for high-capacity and high-rate lithium storage,” *Journal of Materials Chemistry*, vol. 22, no. 7, pp. 2844–2847, 2012.
- [19] E. J. Yoo, J. Kim, E. Hosono, H.-S. Zhou, T. Kudo, and I. Honma, “Large reversible Li storage of graphene nanosheet families for use in rechargeable lithium ion batteries,” *Nano Letters*, vol. 8, no. 8, pp. 2277–2282, 2008.
- [20] X. Huang, H. Yu, J. Chen, Z. Lu, R. Yazami, and H. H. Hng, “Ultrahigh rate capabilities of lithium-ion batteries from 3D ordered hierarchically porous electrodes with entrapped active nanoparticles configuration,” *Advanced Materials*, vol. 26, no. 8, pp. 1296–1303, 2014.
- [21] K. Cao, L. Jiao, H. Liu et al., “3D hierarchical porous α - Fe_2O_3 nanosheets for high-performance lithium-ion batteries,” *Advanced Energy Materials*, vol. 5, no. 4, Article ID 1401421, 2015.



Hindawi

Submit your manuscripts at
<http://www.hindawi.com>

